

# Dendritic cell expression of A20 preserves immune homeostasis and prevents colitis and spondyloarthritis

Gianna Elena Hammer<sup>1</sup>, Emre E. Turer<sup>1</sup>, Kimberly E. Taylor<sup>1</sup>, Celia J. Fang<sup>1,2</sup>, Rommel Advincula<sup>1</sup>, Shigeru Oshima<sup>1</sup>, Julio Barrera<sup>1</sup>, Eric J. Huang<sup>1,3</sup>, Baidong Hou<sup>4</sup>, Barbara A. Malynn<sup>1</sup>, Boris Reizis<sup>5</sup>, Anthony DeFranco<sup>4</sup>, Lindsey A. Criswell<sup>1</sup>, Mary C. Nakamura<sup>1,3</sup>  
& Averil Ma<sup>1</sup>

<sup>1</sup>Department of Medicine, University of California at San Francisco, San Francisco, CA 94143-0451

<sup>2</sup>San Francisco Veterans Affairs Medical Center, San Francisco, CA 94121

<sup>3</sup>Department of Pathology, University of California San Francisco & Pathology Service, VA Medical Center, San Francisco, CA 94121

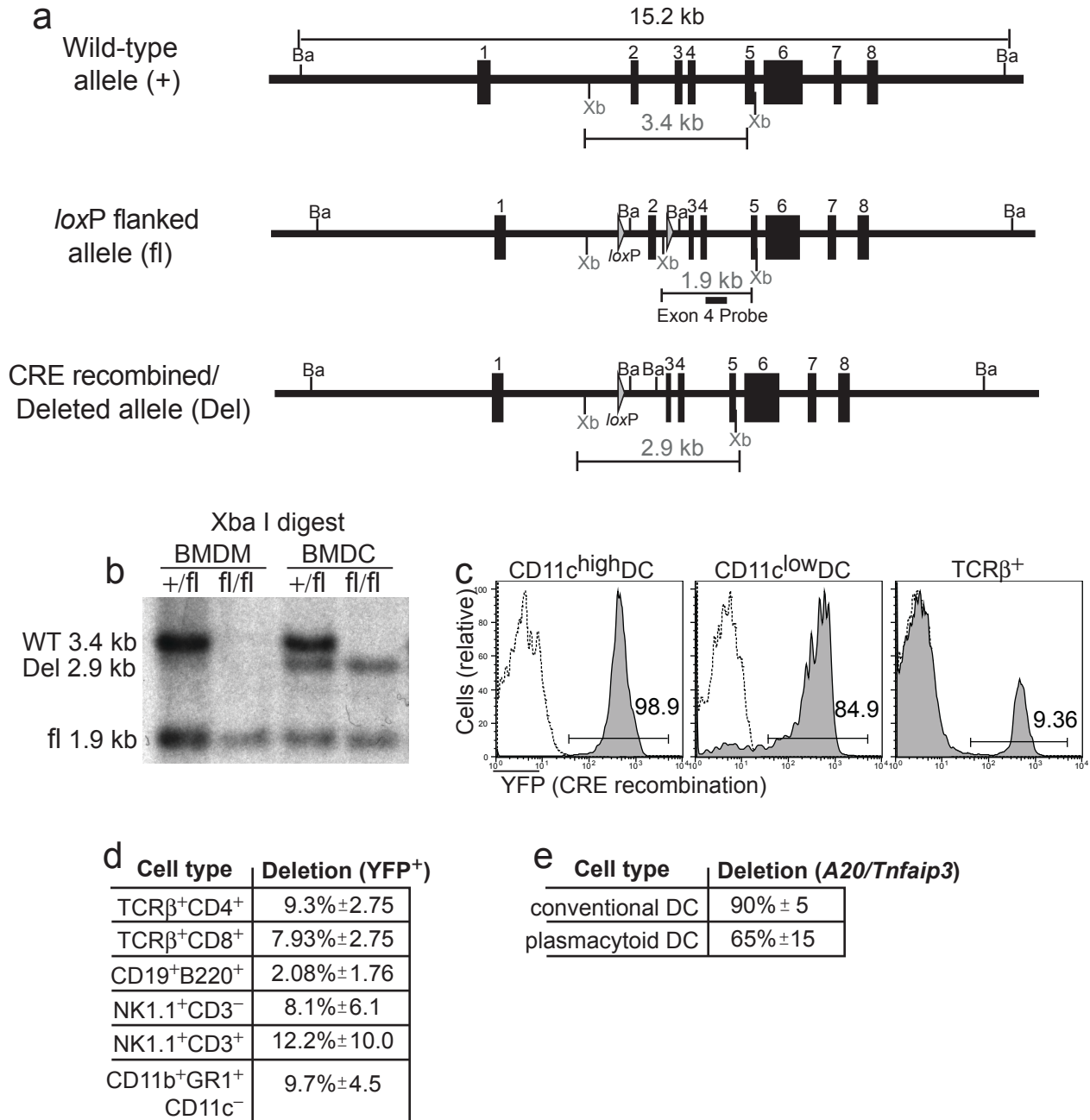
<sup>4</sup>Department of Microbiology and Immunology, University of California at San Francisco, San Francisco, CA 94143

<sup>5</sup>Department of Microbiology and Immunology, Columbia University, NY 10032

Correspondence should be addressed to A.M. (averil.ma@ucsf.edu)  
University of California at San Francisco, 513 Parnassus Ave, S-1057, San Francisco, CA 94143-0451.

**Supplementary Figures**

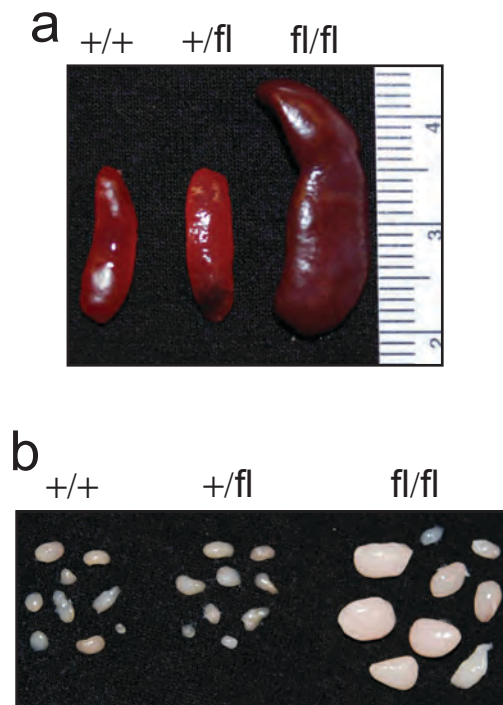
Supplementary Figure 1.



**Supplementary Figure 1. Generation of  $A20^{fl/fl}$  CD11c-Cre mice and specificity of deletion.**

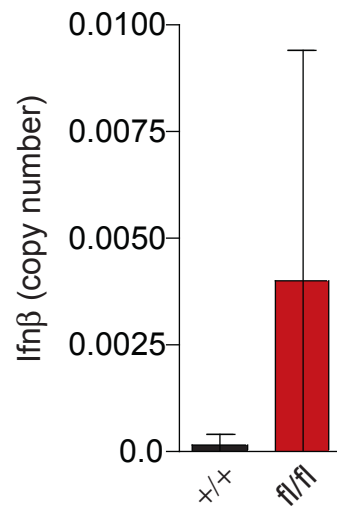
(a) Organization of exons 1-8 of the A20-encoding locus, *Tnfrsf25* in  $A20^{fl/fl}$  mice. Xba I (Xb) restriction sites and the resulting DNA fragment detectable by a probe adjacent to exon 4 are shown for the Wild type (+), *loxP*-flanked allele (“floxed”, fl) and the Cre recombined/deleted allele (Del). (b) Bone marrow derived macrophages (BMDM; 100% F4/80<sup>+</sup>CD11c<sup>-</sup>) and Bone marrow derived dendritic cells (BMDC; 55% CD11c<sup>+</sup>) were harvested after six days of *in vitro* culture. Genomic DNA was digested with Xba I and Cre-mediated deletion of the *loxP* flanked genomic region of exon 2 was analyzed by southern blot using the exon 4 probe shown in (a). (c)  $A20^{fl/fl}$  *Cd11c*-Cre mice were interbred with animals carrying a YFP reporter gene; YFP expression was dependent on CRE-mediated recombination and thus indicates deletion of exon 2 of A20. Shown are representative histograms depicting YFP expression in conventional DCs (CD11c<sup>high</sup>), CD11c<sup>low</sup>DCs, and TCRβ<sup>+</sup> lymphocytes from *Cd11c*-Cre-negative (dashed) and *Cd11c*-Cre-positive (shaded)  $A20^{fl/fl}$  mice. Nearly 100% of DCs were YFP<sup>+</sup> and had deleted A20 as indicated by southern blot (data not shown). The percentage of YFP<sup>+</sup> cells within the indicated cell type is shown in (d). (e) Percent deletion of A20 in sorted splenic populations of conventional DCs (CD11c<sup>high</sup> Ly6C<sup>-</sup> MHC-II<sup>+</sup>) and plasmacytoid DCs (CD11c<sup>low</sup> CD11b<sup>-</sup> Ly6C<sup>+</sup> B220<sup>+</sup>) from  $A20^{fl/fl}$  *Cd11c*-Cre mice. Deletion was assessed using quantitative genomic DNA PCR of A20/*Tnfrsf25* exon 2 (described in<sup>1</sup>) and is relative to that of DCs from control  $A20^{+/+}$  *Cd11c*-Cre mice. Data in (d,e) is averaged from four individual mice.

## Supplementary Figure 2.

**Supplementary Figure 2. A20-deficient DCs induce splenomegaly and lymphadenopathy.**

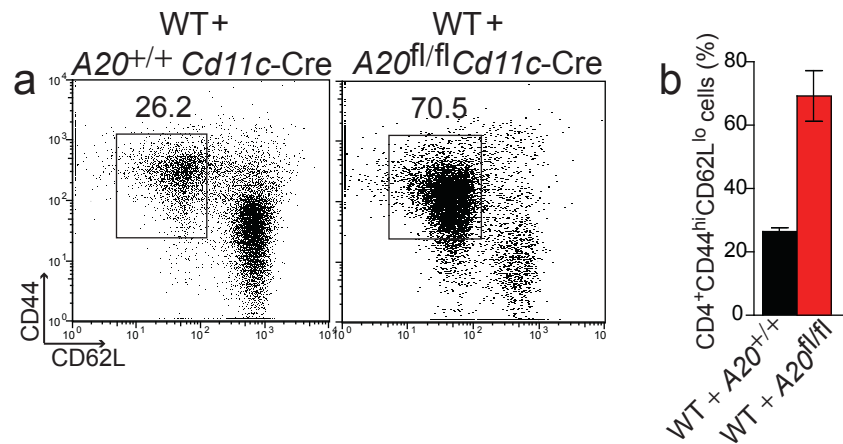
(a) Splens from representative  $A20^{+/+}$  *Cd11c*-Cre mice,  $A20^{+/fl}$  *Cd11c*-Cre mice, and  $A20^{fl/fl}$  *Cd11c*-Cre mice. (b) Lymph nodes from representative  $A20^{+/+}$ ,  $A20^{+/fl}$ , and  $A20^{fl/fl}$  *Cd11c*-Cre mice. Images are representative of more than twenty mice of each genotype between six to ten weeks old.

## Supplementary Figure 3.

**Supplementary Figure 3. A20-deficient DCs produce exaggerated amounts of type I IFN.**

Splenic pDCs were sorted from  $A20^{+/+} Cd11c$ -Cre and  $A20^{fl/fl} Cd11c$ -Cre mice. RNA expression of *Ifnβ*, relative to  $\beta$ -actin, was quantified by QPCR using Taqman Gene Expression Cells to CT kit. Data is averaged from 5 mice.

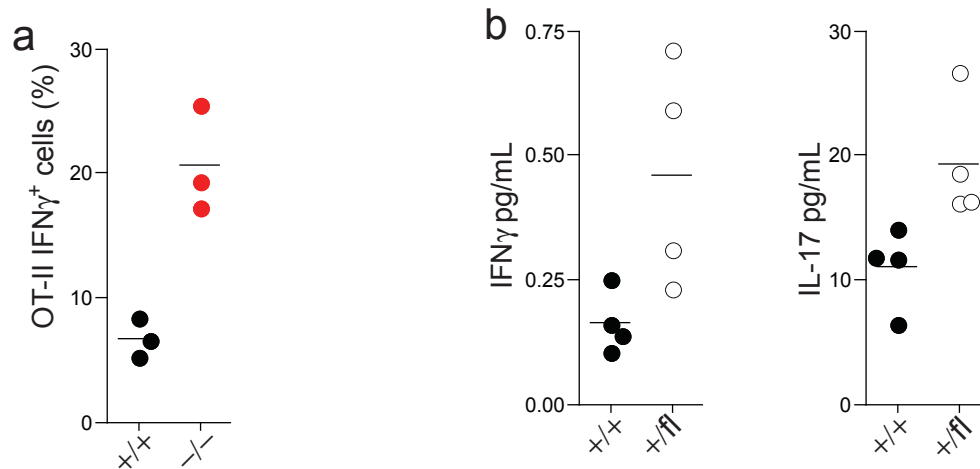
## Supplementary Figure 4.



**Supplementary Figure 4. A20-deficient DCs aberrantly activate T cells in a physiologically dominant fashion over WT DCs.**

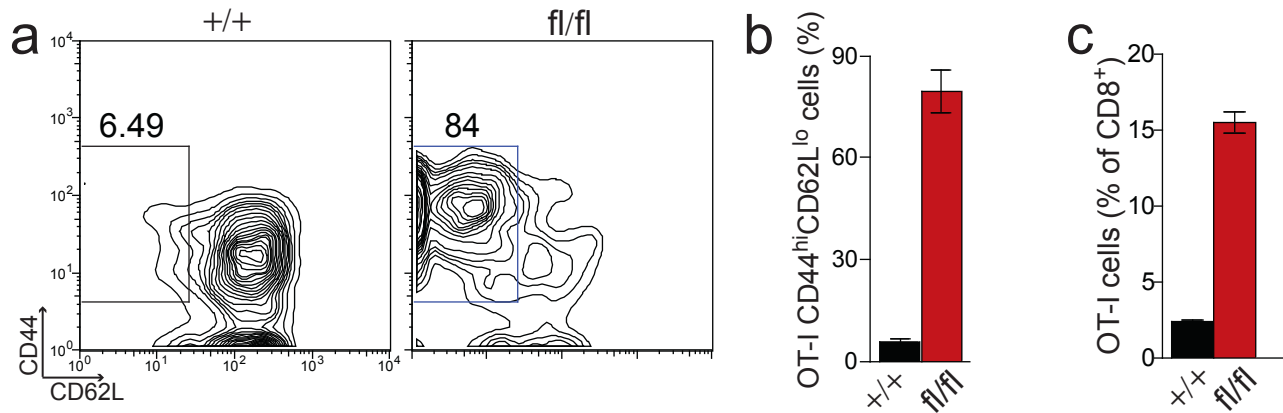
Hematopoietic chimera containing a mixed population of WT and A20<sup>+/+</sup> Cd11c-Cre cells or WT and A20<sup>fl/fl</sup> Cd11c-Cre cells were generated by reconstitution of sublethally irradiated WT mice with congenic A20<sup>+/+</sup> or A20<sup>fl/fl</sup> Cd11c-Cre bone marrow cells. Chimera were analyzed four weeks post irradiation for the percentage of activated CD4<sup>+</sup> T cells (a). The percentage of activated CD4<sup>+</sup> T cells in each chimera is averaged from three independent experiments containing three chimera from each group (b).

## Supplementary Figure 5.

**Supplementary Figure 5. Loss of A20 in dendritic cells enhances T cell activation.**

(a)  $A20^{+/+}$  and  $A20^{-/-}$  BMDCs were sorted by autoMACS and pulsed with 10  $\mu\text{g/mL}$  OVAp for two hours prior to intravenous injection into WT mice containing OT-II T cells. Recipient mice were immunized with  $1 \times 10^6$  antigen-pulsed BMDCs on days zero and day two. Seven days post immunization, spleen cells from recipient mice were restimulated with OVAp and OT-II T cell responses were assayed by intracellular cytokine staining. Shown is the percentage of OT-II T cells making IFN $\gamma$ ; no IL-17 producers were detected. Each dot represents a recipient mouse. (b)  $A20^{+/+}$  *Cd11c*-Cre and  $A20^{fl/fl}$  *Cd11c*-Cre mice were immunized with OVA/complete Freund's Adjuvant (heightened inflammation in  $A20^{fl/fl}$  *Cd11c*-Cre mice precludes their immunization). Two weeks later, lymph node cells from immunized mice were restimulated *in vitro* with 50  $\mu\text{g/mL}$  OVA protein. After 48 hours restimulation, the amount of IFN $\gamma$  and IL-17 in the cell supernatant was assayed by ELISA.

## Supplementary Figure 6.

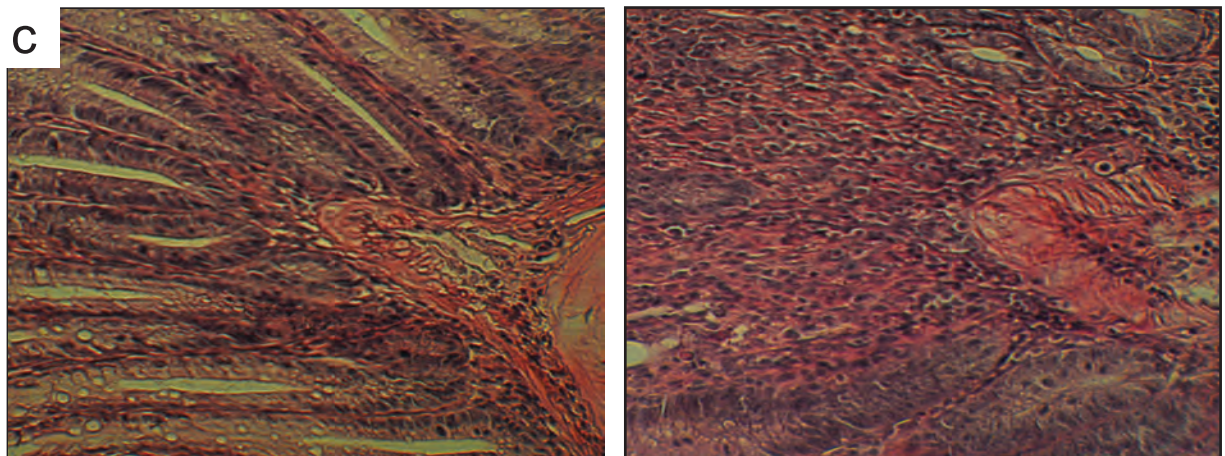
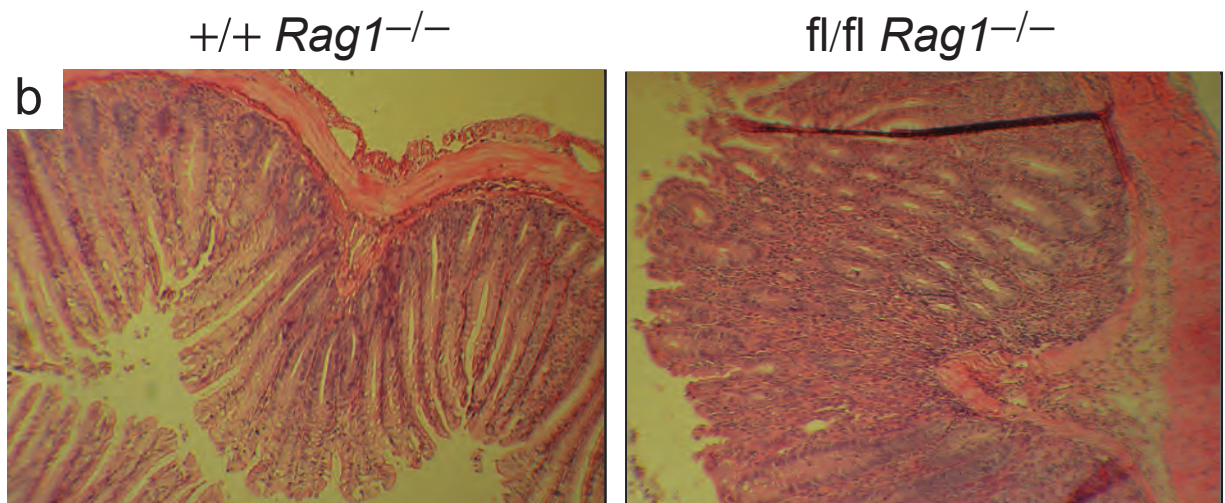
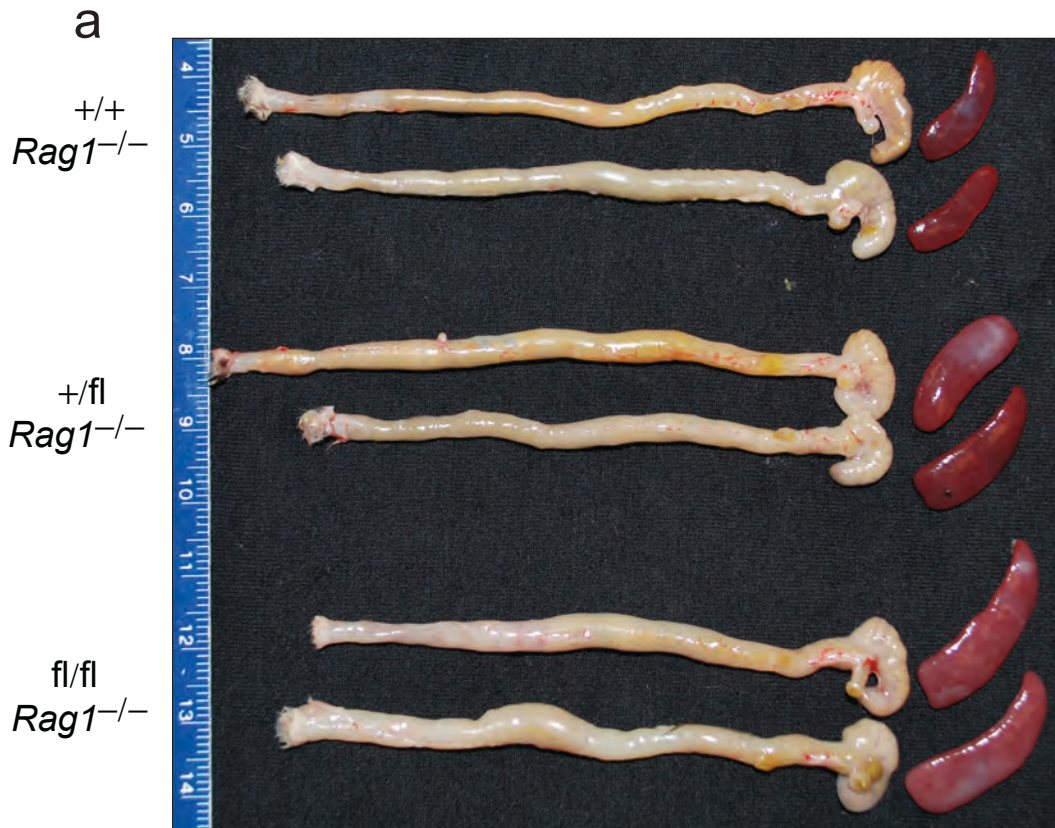


**Supplementary Figure 6. In the absence of antigen, OT-I CD8<sup>+</sup> T cells become activated and expand in *A20<sup>fl/fl</sup> Cd11c-Cre* mice.**

OT-I CD8<sup>+</sup> T cells were adoptively transferred into *A20<sup>fl/fl</sup> Cd11c-Cre* or control *Cd11c-Cre* mice. (a) The percentage of CD44<sup>hi</sup>CD62L<sup>lo</sup> activated OT-I T cells was analyzed nine days post transfer. Activated OT-I T cells in all mice tested (b) and the percentage of OT-I T cells among total CD8<sup>+</sup> T cells (c) is shown. Data includes three recipient mice of each genotype.



Supplementary Figure 7.



**Supplementary Figure 7. A20-deficient DCs rapidly activate and expand T cells to induce colitis.**

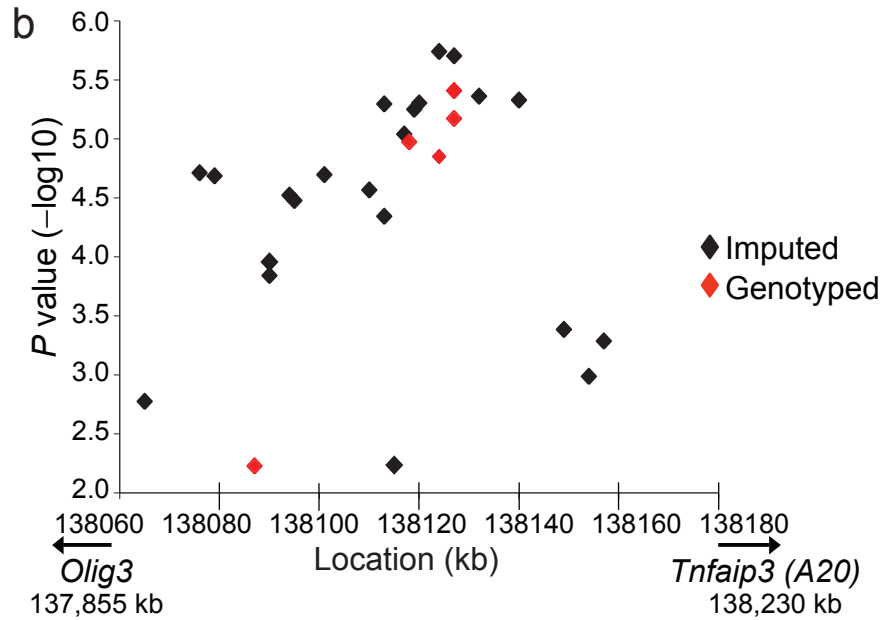
(a) Gross appearance of colons and spleens from  $A20^{+/+}$ ,  $A20^{+/fl}$ , and  $A20^{fl/fl}$   $Cd11c$ -Cre  $Rag1^{-/-}$  mice 24 days post T cell transfer (top to bottom, two mice each). Representative colon histology (b), and lamina propria (c) are shown. Data is representative of two independent experiments including at least two mice per genotype.

## Supplementary Figure 8.

a

		WTCCC, $P < 0.01$ ca=1478, co=2938		
rsid	pos (kb)	type	Add OR	Add $P$
rs2683064	138124	IMP	1.25	1.8E-06
rs7753364	138127	IMP	0.8	2.0E-06
rs6570186	138127	IMP	1.25	2.0E-06
rs7753394	138127	GEN	0.82	3.9E-06
rs12055552	138132	IMP	0.82	4.4E-06
rs9376300	138140	IMP	1.22	4.7E-06
rs9376296	138120	IMP	1.22	5.0E-06
rs999638	138113	IMP	1.22	5.1E-06
rs9389534	138119	IMP	1.21	5.6E-06
rs7773904	138127	GEN	1.21	6.7E-06
rs11961697	138117	IMP	0.82	9.1E-06
rs6927210	138118	GEN	1.21	1.1E-05
rs946227	138124	GEN	1.22	1.4E-05
rs498361	138076	IMP	1.25	1.9E-05
rs650157	138101	IMP	0.81	2.0E-05
rs584794	138079	IMP	0.8	2.1E-05
rs9484087	138110	IMP	0.81	2.7E-05
rs643746	138094	IMP	0.81	3.0E-05
rs508493	138095	IMP	0.81	3.3E-05
rs1538333	138113	IMP	0.84	4.5E-05
rs6917696	138090	IMP	0.82	0.00011
rs6917211	138090	IMP	1.21	0.00014
rs9321631	138149	IMP	0.84	0.00041
rs654039	138157	IMP	1.18	0.00052
rs12212460	138154	IMP	0.82	0.00103
rs9321627	138065	IMP	1.24	0.00168
rs3853402	138115	IMP	1.18	0.0058
rs7766288	138087	GEN	0.81	0.0059

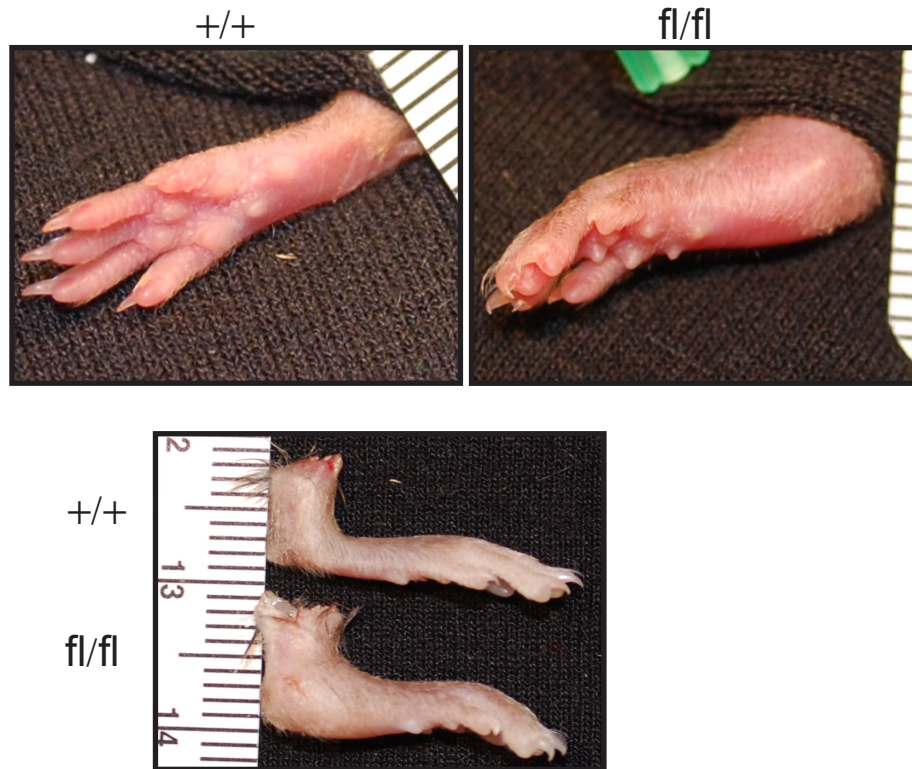
b



**Supplementary Figure 8. Identification of A20/TNFAIP3 SNPs associated with human Crohn's disease.**

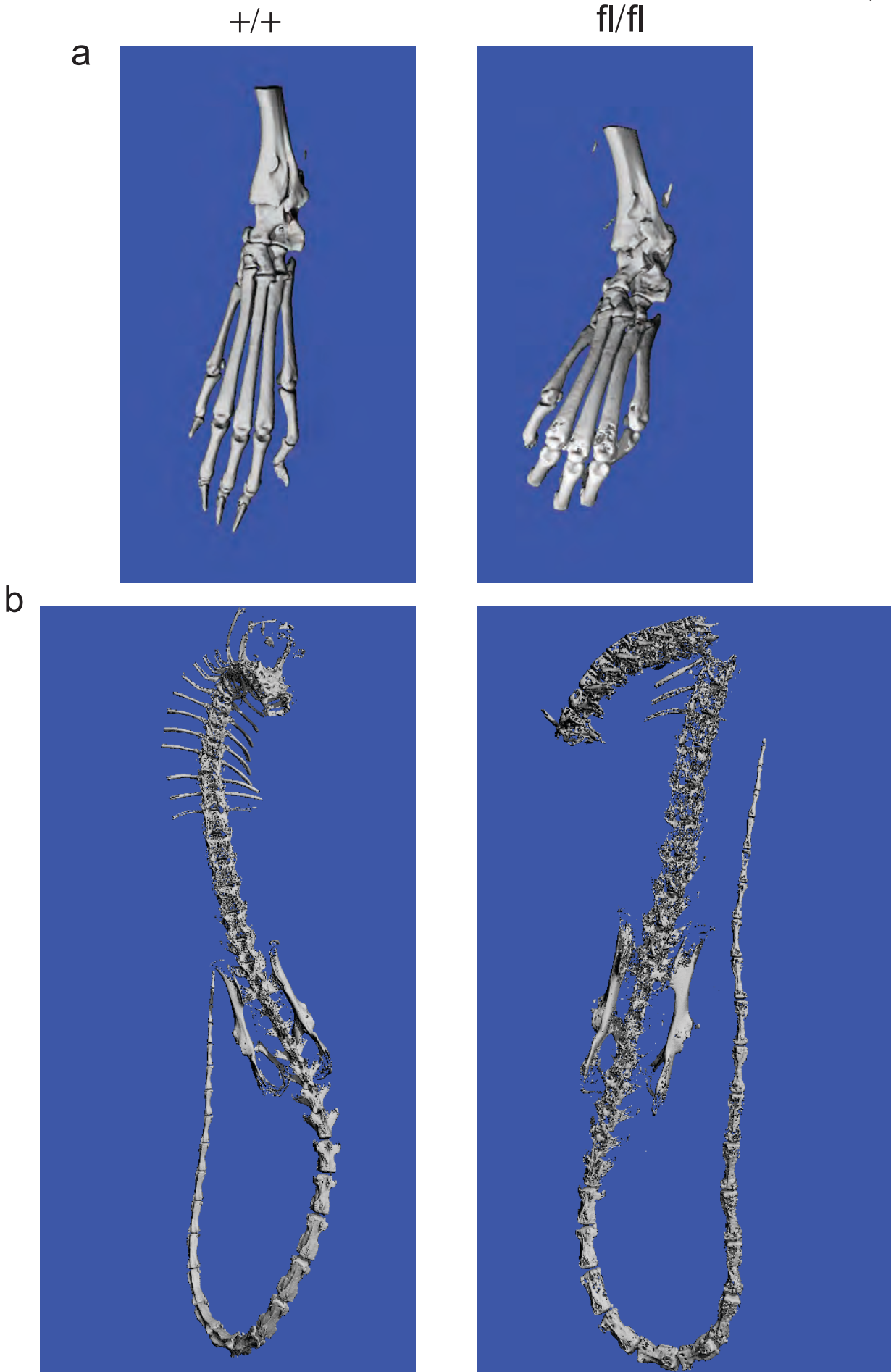
A20/TNFAIP3 and surrounding genomic regions (chr 6: 137,725 -138,800 kb) were analyzed for Crohn's Disease-associated SNPs. After obtaining the publicly-available dataset from WTCCC, we applied quality control thresholds of 90% individual genotyping, 90% SNP genotyping, 5% minor allele frequency; all SNPs had Hardy-Weinberg Equilibrium  $P > 0.01$  in controls. We used IMPUTE<sup>2</sup> to impute up to all HapMap<sup>3</sup> SNPs in A20/TNFAIP3 (chr 6: 138,230 -138,246 kb) and surrounding regions (chr 6: 137,725 -138,800 kb), using the HapMap CEU population as a reference. We retained genotypes imputed (IMP) with a probability of >90% and treated those as absolute genotypes (GEN) in an additive model test. Association was tested using SNPTEST ([www.stats.ox.ac.uk/~marchini/software/gwas/snptest.html](http://www.stats.ox.ac.uk/~marchini/software/gwas/snptest.html)). We performed conditional analysis on the top SNP using Whap<sup>4</sup>. (a) SNP identity (rsid), position (pos), additive odds ratio (OR) and additive  $P$  value of Crohn's Disease-associated SNPs with  $P < 0.01$  in WTCCC. (b) Shown are the  $P$  values plotted by location of imputed (◆) and genotyped (◆) Crohn's Disease-associated SNPs. The upstream location of coding regions for OLIG3 (137,855 kb) and downstream location of A20/TNFAIP3 (138,230 kb) are shown for reference.

Supplementary Figure 9.



**Supplementary Figure 9.  $A20^{fl/fl}$   $Cd11c$ -Cre mice spontaneously develop arthritic disease.**

Representative hindpaws of littermate mice at five months of age; a healthy control and  $A20^{fl/fl}$   $Cd11c$ -Cre mouse suffering acute arthritis is shown. Images are representative of five mice of each genotype.



**Supplementary Figure 10.  $A20^{fl/fl}$  *Cd11c*-Cre mice spontaneously develop spondyloarthritis.**

Skeletons of one year old  $A20^{+/+}$  *Cd11c*-Cre and  $A20^{fl/fl}$  *Cd11c*-Cre mice were analyzed by computed tomography. Shown are representative computed tomography scans of the hindpaw (**a**) and vertebrae (**b**) from  $A20^{fl/fl}$  *Cd11c*-Cre and control mice. Note bone erosions in  $A20^{fl/fl}$  *Cd11c*-Cre mice.

## Supplementary Figure References

1. Tavares, R.M., *et al.* The ubiquitin modifying enzyme A20 restricts B cell survival and prevents autoimmunity. *Immunity* **33**, 181-191 (2010).
2. Marchini, J., Howie, B., Myers, S., McVean, G. & Donnelly, P. A new multipoint method for genome-wide association studies by imputation of genotypes. *Nat Genet* **39**, 906-913 (2007).
3. The International HapMap Project. *Nature* **426**, 789-796 (2003).
4. Purcell, S., Daly, M.J. & Sham, P.C. WHAP: haplotype-based association analysis. *Bioinformatics* **23**, 255-256 (2007).